EUROPEAN FUSION DEVELOPMENT AGREEMENT

EFDA–JET–CP(04)07-08

D.P. Coster, X. Bonnin, A. Chankin, G. Corrigan, S.K. Erents, W. Fundamenski, J. Hogan, A. Huber, A. Kallenbach, G. Kirnev, A. Kirschner, T. Kiviniemi, S. Kuhn, A. Loarte, J. Lönnroth, G.F. Matthews, R.A. Pitts, S. Sipiläg, J. Spence, J. Strachan, F. Subba, E. Tsitrone, D. Tskhakaya, S. Wiesen, M. Warrier, M. Wischmeier, R. Zanino and JET EFDA Contributors

Integrated Modelling of Material Migration and Target Plate Power Handling at JET

Integrated Modelling of Material Migration and Target Plate Power Handling at JET

D.P. Coster[1], X. Bonnin[2], A. Chankin[1], G. Corrigan[3], S.K. Erents[3], W. Fundamenski[3], J. Hogan[4], A. Huber[5], A. Kallenbach[1], G. Kirnev[6], A. Kirschner[5], T. Kiviniemi[7], S. Kuhn[8], A. Loarte[9], J. Lönnroth[7], G.F. Matthews[3], R.A. Pitts[10], S. Sipiläg[7], J. Spence[1], J. Strachan[11], F. Subba[12], E. Tsitrone[2], D. Tskhakaya[8], S. Wiesen[5], M. Warrier[13], M. Wischmeier[10], R. Zanino[12] and JET EFDA Contributors*

[1]Max-Planck-Institut f¨ur Plasmaphysik, EURATOM Association, D-85748 Garching, Germany
[2]Association Euratom-CEA, CEA/DSM/DRFC, CEA-Cadarache, F-13108 St-Paul-Lez-Durance, France
[3]EURATOM/UKAEA Fusion Association, Culham Science Centre, Abingdon Oxon OX14 3DB, UK
[4]Oak Ridge National Laboratory, Oak Ridge, USA
[5]Institut für Plasmaphysik, FZ Jülich, EURATOM Association, Jülich, Germany.
[6]Kurchatov Institute, Moscow.
[7]Helsinki University of Technology, Association Euratom-Tekes, Finland.
[8]Department of Theoretical Physics, University of Innsbruck, Innsbruck, Austria.
[9]EFDA, Garching, Germany.
[10]CRPP, Association EURATOM-Confédération Suisse, EPFL, Lausanne, Switzerland.
[11]Princeton Plasma Physics Laboratory, Princeton, USA.
[12]Politecnico di Torino, Torino, Italy.
[13]Max-Planck-Institut f¨ur Plasmaphysik, EURATOM Association, D-17491 Greifswald, Germany.
** See annex of J. Pamela et al, "Overview of JET Results ",*
(Proc.20 th IAEA Fusion Energy Conference, Vilamoura, Portugal (2004).

Preprint of Paper to be submitted for publication in Proceedings of the
20th IAEA Conference,
(Vilamoura, Portugal 1-6 November 2004)

ABSTRACT.
The complexity of the tokamak edge and Scrape-Off Layer (SOL) region is such that extrapolation to ITER requires modelling to be pursued through the integration of a number of edge codes, each of which must be thoroughly tested against results from present day machines. This contribution demonstrates how the edge modelling effort at JET is focused on such an approach by considering two examples, target power loading and material erosion and migration, the understanding of which are crucial issues for ITER.

We start with an overview of JET edge modelling in the areas of material migration and target power handling. Then we concentrate on some new modelling results related to drifts in JET, and discuss the implications for material migration. Finally the implications of an alteration in the model for C recycle are explored. The features of the codes used are summarized in [1].

1. TARGET POWER HANDLING.

Engineering constraints on the ITER divertor targets impose a limit on the maximum peak power flux in steady state, whilst ablation or melting limits constrain the peak energy loss during ELMs. Power exhaust is found to involve an interplay between kinetic effects (ion orbit loss) responsible for energy transport into the SOL, and collisional processes (classical ion conduction) which dominate energy transport in the SOL and determine the magnitude and scaling of the deposited power profiles. This conclusion has been reached with the help of extensive ASCOT modelling of ion orbit loss, together with fluid modelling of energy transport in the SOL and important data provided by recent analysis of the reversed B-field experiments[2].

1.1. ELMS.

A different modelling problem is posed by ELMs, for which the non-linear evolution of the instability on closed field lines is not yet well understood([3] and references therein). Some success has been achieved in understanding the linear phase of the ELM in terms of a ballooning/peeling model. A simplified 1d model (JETTO) of the closed field line region in the edge plasma has been used to study possible ELM dynamics. Some of the experimentally observed trends have been duplicated. Concerning the nature of the heat pulse that crosses the separatrix and its impact on the targets, ELMs in JET have been modelled using two different approaches. In the first, the COCONUT code (the combination of the 1d JETTO core code and EDGE2D-NIMBUS), has been used to model the impact of ELMs both on the core plasma and the SOL. Separately, the EDGE2D-NIMBUS[4] and SOLPS5 packages has been applied to model the detail of particular ELMs and to study the mitigating effects of N, Ne and Ar radiation by simulating the ELM-affected region of the core plasma in addition to the SOL.

These simulations have shown that, while it is not possible to buffer large ELMs, their effects can be somewhat mitigated by decreasing the average power crossing the separatrix between ELMs (thus lowering the inter-ELM average target temperature) and potentially by changing the ELM dynamics on closed field lines[5].

Simulation of experimental data for particular ELMs[6] has produced a good match both for the energy loss from the main plasma (by the appropriate choice of transport multipliers and their spatial

and temporal domain), and the power seen at the target, figure 1. A discrepancy has been found, however, between the code prediction and experimentally observed Dα emission. Rather symmetric Dα emission from the two divertors is seen in the code, while experimentally a strong asymmetry favouring the inner target is observed. This is an indication that hydrocarbon layers, thought to be present on the inner target, may be producing greater neutral desorption at the ELM impact. Such effects are not yet included in the code simulations. At the outer target, where layers are not normally present in JET, code and experiment are in good agreement.

Kinetic effects (in the form of parallel electron and ion heat flux limiters), seen to be important in the SOLPS/EDGE2D code/code benchmarks [7], are expected to play an even stronger role during ELM events. In determining some aspects of the physics, they assume a dominant role. Of particular additional importance would be the effect of hot electrons changing the sheath boundary condition at the target, and parallel heat transport deviating strongly from that given by the fluid expressions (even with flux limiters) [8]. An effort has been launched to investigate this using PIC simulations including the effects of strong recycling in the pre-ELM phase.

Since most ITER simulations to-date have been for steady state, the ELM modelling is now being extended to ITER. Many details of the ELM event are complex and not yet understood. However, the transport multiplier approach in fluid models, in conjunction with kinetic analysis does seem to offer a reasonable description of the heat pulse propagation and many aspects of edge profile evolution.

1.2. INTEGRATED PLASMA/PLATE MODELLING.

Given the relative success of the plasma simulations, a thermal model of the target is being developed so that target erosion at the ablation limit can be evaluated self-consistently.

Early results (for steady-state) of the predicted target plate temperature are shown in figure 2 where SOLPS D+C+He fluid neutral simulations of a power scan from 2MW to 4MW with a feedback controlled upstream separatrix electron density of $1.5\times10^{19}m^{-3}$ were performed. A target thickness of 4cm with a back-plate cooled to 373K and thermal diffusivities and heat capacities typical of the CFC's used in the JET targets, were used. In these calculations, the plate temperature affected the chemical sputtering yield[1], with average chemical sputtering yields for the two targets shown in table 1.

2. MATERIAL MIGRATION.

The lifetime of the ITER target is critically dependent on the rate of material erosion, both in the quiescent phase and during transients and is largely determined by the target power loading described above. If C is chosen as the target material, the issue of its erosion and subsequent deposition becomes important — since T is co-deposited with the C and there is a limit on the amount of T allowed in the machine. It is therefore important to test the existing models of this process on existing machines, before applying them to ITER.

At JET carbon flakes are observed mainly at the inner target, pointing to an asymmetry of C deposition[9] of about 97:3 in favour of the inner target (based on the tritium measured). In addition,

[1] *Roth's chemical sputter yield formula from the 11th EFPW in Heraklion (Dec. 2003) was used; it contains both a temperature and a flux dependence.*

the interpretation of infra-red thermography measurements requires the assumption of a thin, low heat conductivity layer on the inner target, likely associated with carbon deposition [10,11]. A recent experiment at JET found that when ^{13}C was introduced via a methane gas puff at the top of the machine, most (99%) of the ^{13}C found at the targets was seen at the inner divertor, [12].

A number of approaches have been taken to incorporate these observations into edge models. Work by Coad *et al.*[9] showed that if they assumed: enhanced C erosion from the vacuum vessel, an added flow towards the inner target and enhanced carbon recycling at the inner target, then Monte-Carlo modelling of the impurity ions against a fluid main plasma was able to produce a strong deposition on the louvers near the inner target.

With "standard" assumptions, the 2d fluid plasma codes cannot reproduce the experimentally observed predominance of C deposition at the inner target in JET (or, perhaps relatedly, of the observed flows measured at the top of the machine).

Using the codes with drift terms switched on does improve the situation somewhat, but still leaves differences. In an effort to improve the match, additional effects have been suggested and are being tested: (a) the addition of an external momentum source [EDGE2D-NIMBUS] (Matthews *et al.*[13] investigated ion orbit loss interactions as an explanation of the observed Mach flows and found the effects to be small, though in the right direction; Strachan *et al.*[14] has looked in more detail at imposing an additional force on the particles in the SOL and found that these changes did not significantly change the screening of impurities); (b) the possibility that a component of the observed Mach flows might be caused by the probe itself [EDGE2D-NIMBUS][15]; (c) the effects of transport ballooning [EDGE2D-NIMBUS & SOLPS] ([16] and discussed below); (d) the effects of a drift in the major radius direction [EDGE2DNIMBUS] (Kirnev *et al.*[17] assumed an *ad hoc* drift in the grad-R direction and were able to reproduce the observed flows); (e) additional atomic physics related to the erosion/deposition balance [SOLPS] (discussed below). All of the EDGE2D-NIMBUS have been published elsewhere, and the SOLPS results are discussed in the following section.

2.1. RECENT SOLPS RESULTS IN EXAMINING THE ROLE OF DRIFTS IN DETERMINING FLOWS AT JET.

On JET measurements from reciprocating Langmuir probes positioned at the top of the machine, just outside of the magnetic axis (approximately at the one o'clock position) have revealed[15] a peak flow of approximately Mach 0.5 towards the inner divertor in the forward field case (ion grad-B drift direction towards the lower X-point), and approximately stagnant flow at this position for the reversed field case, giving a peak forward/reversed field Mach difference of 0.5. Modelling with EDGE2D-NIMBUS has shown a forward/reversed field Mach difference in the right direction, but with a magnitude that is too small (by a factor 5–10)[15]. SOLPS (B2-Eirene) modelling shows a somewhat larger forward/reversed field Mach difference, particularly when impurities are included (compared to the benchmark cases in [7]). Figure 3 shows the predicted Mach number for a number of SOL flux tubes as a function of poloidal position, and figure 4, left, shows the predicted Mach number at the JET reciprocating probe position for D + ^{12}C + ^{13}C + He simulations of low power (2.5MW) low

density (upstream separatrix electron density of $0.5\times10^{19}\mathrm{m}^{-3}$, feedback controlled by a D gas puff) JET discharges. The simulations show a flow directed towards the inner target of M = 0.15 for the forward field case, M = 0.1 towards the outer target for the reversed field case, and a value close to 0 for simulation without drifts.

Increasing amounts of transport ballooning (where the localtransport coefficient was scaled by $(B_{ref}/B_{\mathrm{loc}})^{\alpha}$) is observed to shift the "base" value of the Mach number from approximately M = 0 to M = 0.25 directed towards the inner target, figure 4, right. (Combining drifts and ballooning produces a roughly additive effect in the case investigated to date). The reason that SOLPS seems to produce a higher Mach flow than EDGE2D-NIMBUS is not clear yet – these calculations were done with a somewhat higher power and lower electron density than in [15], both of which would tend to increase the drift effects. Benchmarking of the two codes against each other has started (for the non-drift case, see [7]).

In section 2.3, the effect of these drifts on material migration is examined.

2.2. THE ROLE OF DRIFTS ON POWER ASYMMETRIES AND THE OHMIC DENSITY LIMIT.

The drifts, as expected, have an impact on the target power deposition. Starting with the $0.5\times10^{19}\mathrm{m}^{-3}$ upstream separatrix electron density, a density ramp was performed by removing the feedback control on the separatrix density and the pumping while puffing D.

Figure 5, left, shows the upstream separatrix electron density as a function of time during a density ramp for simulations without drifts ("NONE"), and with drifts with ion drift direction towards ("FWD") and away from ("REV") the X-point. The simulations reproduce the observed ([18]) lower density limit in the reversed B field case. Figure 5, right, shows the total D+ particle fluxes to the targets as a function of the upstream separatrix electron density. As expected, we see an initial increase of the flux to the targets with increasing density, followed by saturation, and then a strong decrease at approximately constant upstream density.

Figure 6, left, shows the predicted total power to the targets as a function of the upstream separatrix electron density. At low densities, the forward field case has more power going to the outer target than the inner, but the asymmetry decreases at higher densities. The asymmetries are even larger if only the electron contribution is plotted, figure 6, right. This can be understood in terms of the transition from conducted power flows (at low densities, and in particular via the electrons), to convected power flows (at the highest densities, significantly by the convected energy of the 13.6

2.3. THE EFFECT OF DRIFTS ON $^{12}C + ^{13}C$ DEPOSITION.

In order to investigate the observations discussed above in section 2, the runs described in section 2.1 (plus additional runs) were analysed to look at the flows of $^{12}\mathrm{C}$ and $^{13}\mathrm{C}$ to the two divertors.

Neither drift effects nor transport ballooning – despite their effects on the Mach number – had a strong effect on the observed $^{12}\mathrm{C}$ target flux asymmetry, and showed only a slightly larger (but still small) effect on the 13C target flux asymmetry. Varying the position of the D gas puff was also largely ineffective. Density was observed to strongly affect the 13C target flux asymmetry, with a weaker

effect on the ^{12}C target flux asymmetry, as can be seen in figure 7 which shows (left) the fraction of ^{12}C and (right) the fraction of ^{13}C absorbed at the inner target to that absorbed at both targets. (The initial points at the lowest density reflect the previously quoted dependence on drifts alone).

At higher densities, the flux fraction of ^{12}C absorbed at the inner target rises to about 70% (still low compared to the experimentally observed 97%). For the ^{13}C, the rise occurs at lower density, and to higher inner target absorption fractions – not too far from the experimentally observed fraction of 99%.

2.4. A MODIFIED RECYCLING MODEL FOR C.

In order to try and find a possible explanation for the observed ^{12}C asymmetry ration of 97%, the effects of changing the C recycling model in the code were explored. All the runs reported above used physical and chemical sputtering as the source of C, and assumed that C incident on a surface was absorbed.

Experimental observations and code simulations ([19] and references therein) have indicated an influence of the electron temperature in determining whether a surface exposed to a combined flux of D and C is erosion or deposition dominated. For a given C concentration, a transition is made from net deposition to net erosion as the electron temperature is increased, with this critical temperature increasing with increasing C concentration.

To mimic the above effect, a model was added to Eirene in SOLPS to change the recycling model used if the local electron temperature was above a specified value so that the C would recycle. This model does not preclude enhanced erosion of deposited films – provided such eroded material is re-deposited locally. It is likely that just such a mechanism exists and is responsible for moving the C deposited at the inner target to the inner louvers; in these simulations we are interested in the global flows of C.

In table 2, we show the ratio of the C absorbed on the inner target to the total absorbed C at both targets. The first row, with the label "Crec = 0" reflects the data plotted in figure 7 at the lowest density, with the default model of incident C being absorbed. The second row, "C^{13}rec = 1", enforced complete recycling of ^{13}C. The next two cases switched on recycling above an edge electron temperature of $10eV$ for just ^{13}C and for both C species, respectively. The last two cases used a cut-off temperature of $5eV$ for the switch-over from complete absorption to recycling.

Concentrating first on the "drifts" equals "no" column for ^{12}C and on the "Crec = 0", "Crec = 10eV" and""Crec = 5eV" cases, we see an increase of the ^{12}C fractional deposition at the inner target from 46% through 57% to 85%. The effect of drifts is now pronounced — taking the "Crec=10eV" case, the forward field case has 95% deposition at the inside, with only 5% at the outside2; and the reversed field case has a 45% absorption fraction at the inner target, with 55% at the outer target. Experimentally, under these circumstances, some sort of film seems to grow at the outside, which would be supported by these calculations. (It should be noted that the effect of the modified recycling model is strongest at lowish densities, when the target plasma temperature asymmetry is largest.) The asymmetry for the externally puffed 13C is not as pronounced, though shows similar trends as for the intrinsically produced 12C.

3. DISCUSSION.

In this paper we gave an overview of the different approaches that are being used to try and understand the issues of target power handling and material migration. Of particular interest, and the emphasis of this paper, are issues related to integrated modelling of the edge plasma.

Early results from a self-consistent calculation where the plasma conditions affected the target plate temperature, and thereby the chemical sputtering of C from the plate, which then affected the plasma conditions, were presented.

The important issue of material migration was then examined. The existing edge codes have had difficulties matching the experimentally measured Mach flows in the edge plasma, but even when the agreement is reasonable, these drift related flows are not observed to have a strong effect on material migration in the simulations. At increased densities, a strong rise was seen in the predicted 13C flux asymmetry to the targets, approaching the experimentally observed 13C flux asymmetry.

None of the "usual" effects were observed to give a"12C flux asymmetry approaching that seen in the experiment. A simple extension to the C recycling model used in the code was proposed, and shown to give — under the conditions examined — —12C flux asymmetries to the targets approaching (or exceeding) the experimentally observed value. This model is still relatively crude, but, incrementally, adds a feature that has been observed experimentally and in (local) kinetic calculations. The magnitude of the effect seen with this model strongly suggests that additional work in this area is necessary. Further work is also necessary to explore in more detail the implications of this model, in particular for ITER; also the model needs to be extended to include the self-consistent treatment of the plate temperature, which also has an effect on material erosion.

REFERENCES

[1]. Coster, D. et al., J. Nucl. Mater. **313–316** (2003) 868.

[2]. Fundamenski, W. et al., Effect of *B*° — Ñ*B* direction on SOL energy transport in JET, presented at the 2004 Plasma Surface Interactions Conference and submitted to Journal of Nuclear Materials.

[3]. Becoulet, M. et al., Edge Localised Modes control: Experiment and theory, presented at the 2004 Plasma Surface Interactions Conference and submitted to Journal of Nuclear Materials.

[4]. Kallenbach, A. et al., Plasma Phys. Controlled Fusion **46** (2004) 431.

[5]. Monier-Garbet, P. et al., Assessment of the use of injected impurities for heat flux mitigation in JET ELMy H-modes., in *Europhysics Conference Abstracts (CD-ROM, Proc. of the 30th EPS Conference on Controlled Fusion and Plasma Physics, St. Petersburg, 2003)*, volume 27B, Geneva, 2003, EPS.

[6]. Subba, F. et al., Modeling JET ELMs with the SOLPS edge plasma code, in *Europhysics Conference* Abstracts (CD-ROM, Proc. of the 30th EPS Conference on Controlled Fusion and Plasma *Physics, St. Petersburg, 2003)*, volume 27B, Geneva, 2003, EPS.

[7]. Coster, D. et al., Benchmarking tokamak edge modelling codes, presented at the 2004 Plasma Surface Interactions Conference and submitted to Journal of Nuclear Materials.

[8]. Tskhakaya, D. et al., Kinetic simulations of the tokamak scrape-off layer, invited talk given at Theory of Fusion Plasmas, Joint Varenna-Lausanne InternationalWorkshop, Varenna, Italy, August 29–September 3, 2004; To be published in the conference proceedings.
[9]. Coad, J. et al., J. Nucl. Mater. **290–293** (2001) 224.
[10]. Andrew, P. et al., Outer divertor target impurity deposition suring reversed magnetic field operation in JET, presented at the 2004 Plasma Surface Interactions Conference and submitted to Journal of Nuclear Materials.
[11]. Corre, Y. et al., Inner and outer power and energy asymmetries during L-mode power staircase pulses with forward and reversed magnetic field, in *Europhysics Conference Abstracts (CDROM, Proc. of the 31st EPS Conference on Controlled Fusion and Plasma Physics, London, 2004)*, Geneva, 2004, EPS.
[12]. Strachan, J. et al., EDGE2D simulations of JET 13C migration experiments, in *Europhysics* Conference Abstracts (CD-ROM, Proc. of the 31st EPS Conference on Controlled Fusion and *Plasma Physics, London, 2004)*, Geneva, 2004, EPS.
[13]. Matthews, G. et al., J. Nucl. Mater. **313–316** (2003) 986.
[14]. Strachan, J. et al., Methane screening in JET reverse field experiments, presented at the 2004 Plasma Surface Interactions Conference and submitted to Journal of Nuclear Materials.
[15]. Erents, S. et al., Plasma Phys. Controlled Fusion **46** (2004) 1757.
[16]. Pitts, R. et al., Edge and divertor physics with reversed toroidal field in JET, presented at the 2004 Plasma Surface Interactions Conference and submitted to Journal of Nuclear Materials.
[17]. Kirnev, G. et al., EDGE2D code simulations of SOL flows in JET, presented at the 2004 Plasma Surface Interactions Conference and submitted to Journal of Nuclear Materials.
[18]. Huber, A. et al., The effect of field reversal on the JET MkIIGB-SRP Divertor performance in L-mode density limit discharges, presented at the 2004 Plasma Surface Interactions Conference and submitted to Journal of Nuclear Materials.
[19]. Ohya, K. et al., Physica Scripta **T111** (2004) 138.

P_{SOL}	Average Erosion yield	
	Inner Divertor	Outer Divertor
2.0MW	4.94 (10^{-6})	3.64 (10^{-3})
2.5MW	5.67 (10^{-6})	4.09 (10^{-3})
3.0MW	7.93 (10^{-5})	4.76 (10^{-3})
4.0MW	9.33 (10^{-4})	5.60 (10^{-3})

JG05.83-12c

Table 1: Average erosion yields (i.e chemically eroded C flux/incoming (D^0,D^+) flux) for the cases with target temperatures plotted in figure 2.

	^{12}C			^{13}C		
Drifts	FWD	NONE	REV	FWD	NONE	REV
Crec = 0	0.62	0.46	0.40	0.30	0.35	0.37
C13rec = 1	0.58	0.45	0.47	–	–	–
C13ec = 10eV	0.62	0.47	0.41	0.53	0.45	0.44
Crec = 10eV	0.95	0.57	0.45	0.64	0.45	0.38
C13rec = 5eV	0.63	0.46	0.45	0.64	0.50	0.34
Crec = 5eV	1.14	0.85	0.48	0.81	0.54	0.41

JG05.83-13c

Table 2: Fraction of the C absorbed at the inner target (incoming-outgoing) to that absorbed at both targets for various assumptions about C recycling. Based on T analysis, the ^{12}C asymmetry is approximately 0.97 and from the ^{13}C gas puff experiment, the ^{13}C asymmetry is approximately 0.99.

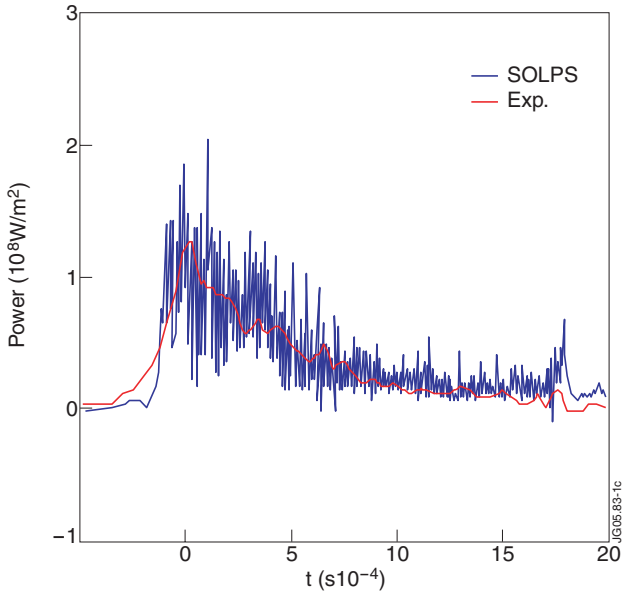

Figure 1: Comparison of the power flux to the outer target on JET between the experimental measurement and a SOLPS simulation.

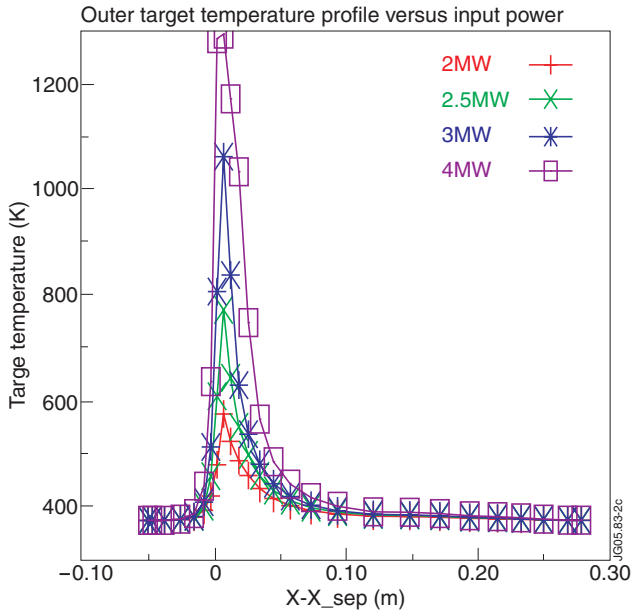

Figure 2: Steady state temperatures for JET-like target plates.

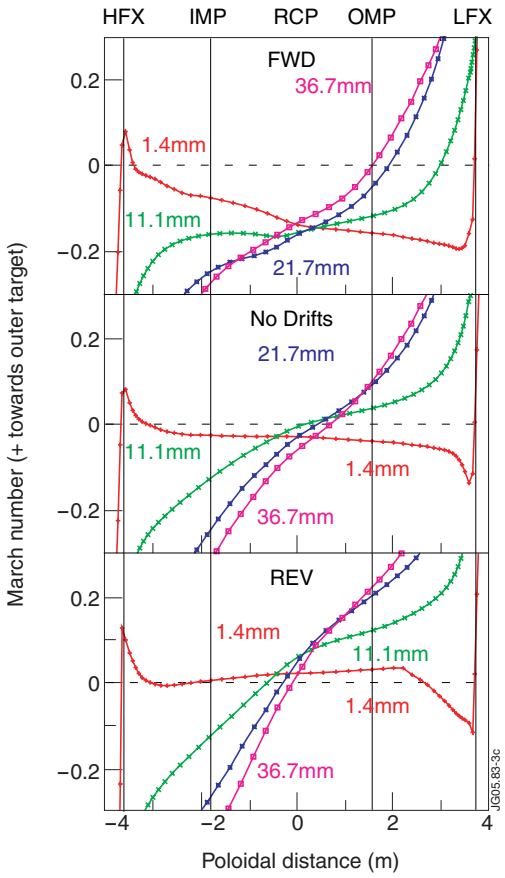

Figure 3: Mach number plotted as a function of poloidal distance for four flux tubes, at 1.4mm, 11.1mm, 21.7mm and 36.7mm from the separatrix (measured at the outer midplane), for the cases with forward field, no drifts and reversed field (top to bottom). Also marked are the approximate positions of the X-point (on the high field side, HFX), inner Mid-lane (IMP), reciprocating probe position (RCP), outer midmlane (OMP) and the X-point again (low field side, LFX); the inner target is on the left and the outer target on the right.

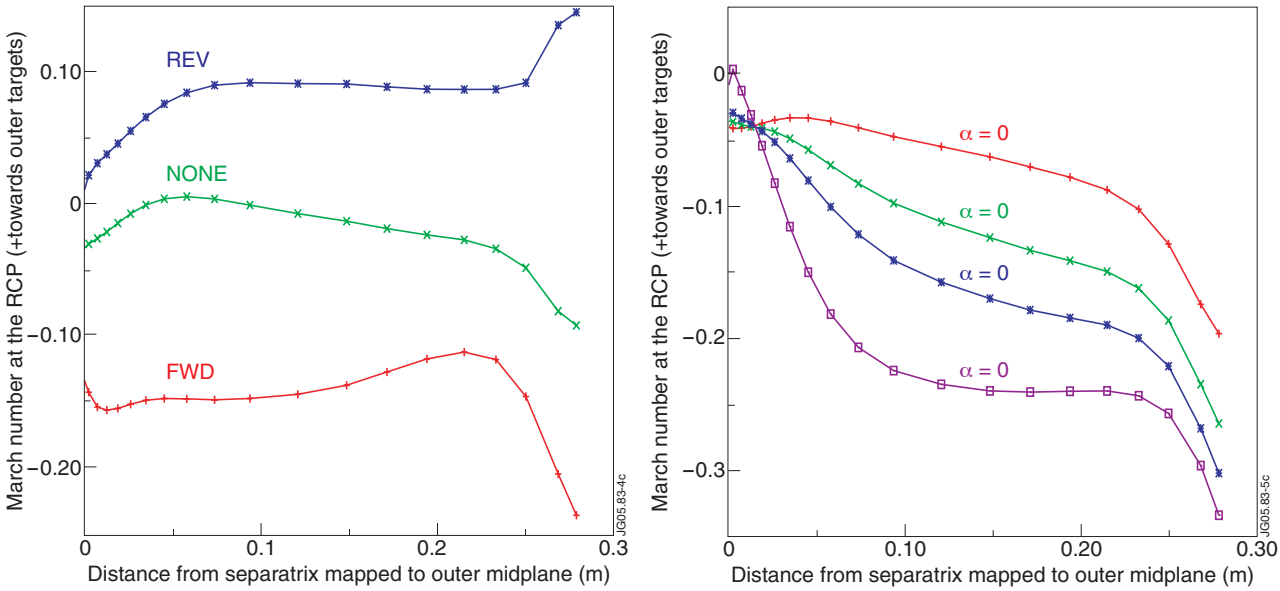

Figure 4: Left: Predicted Mach number at the position of the JET reciprocating probe position for forward, no and reversed drift SOLPS simulations with D + ^{12}C + ^{13}C + He. Right: Effect of transport ballooning on the predicted Mach numbers at the JET reciprocating probe position for cases without drifts but differing amounts of transport ballooning. (Compare to [15], figure 6.)

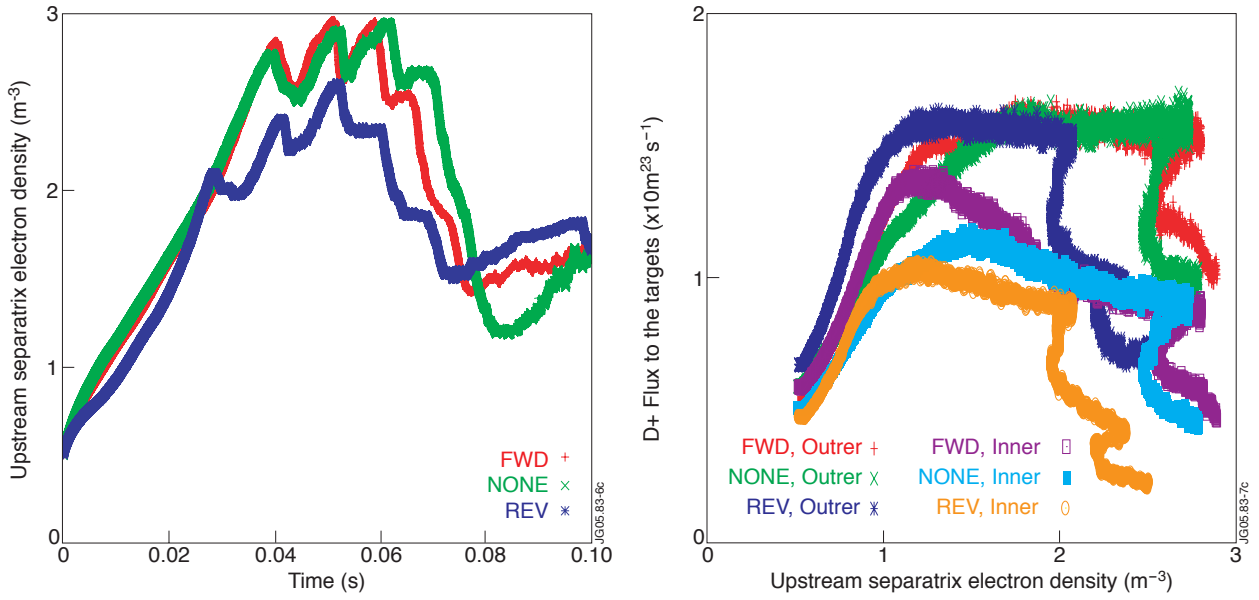

Figure 5: Left: upstream separatrix electron density as a function of time for forward field, no drifts, and reversed field cases; Right: total target D^+ particle fluxes to the inner and outer targets.

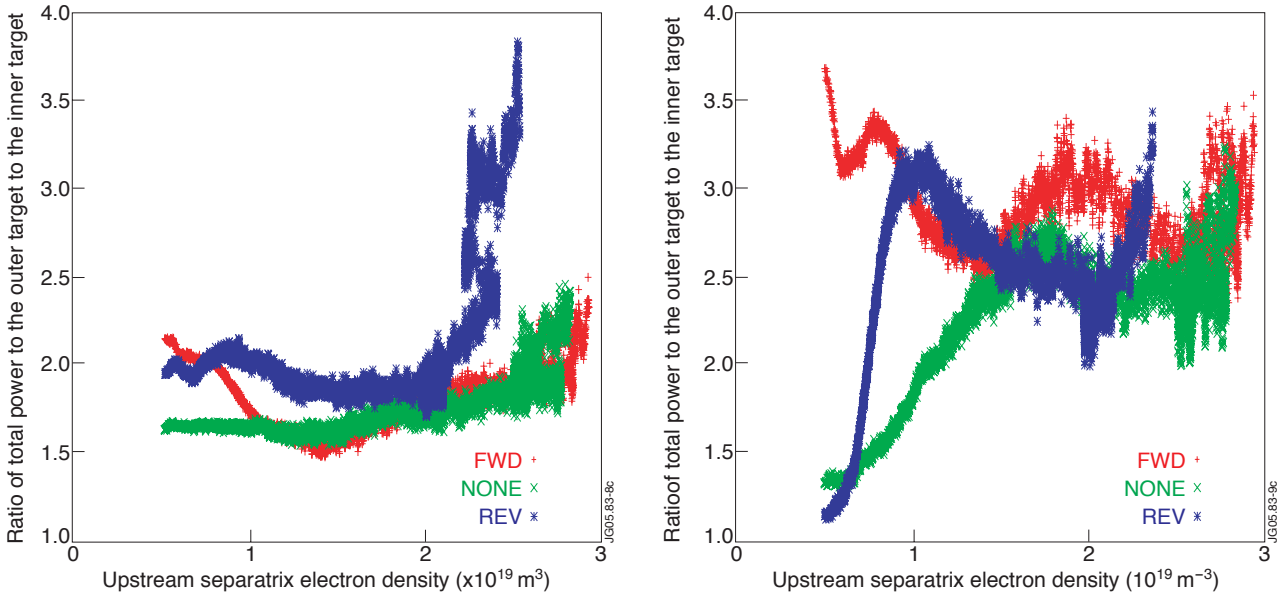

Figure 6: Ratio of total (left) and electron (right) power to the outer target to the inner target for the cases in figure 5.

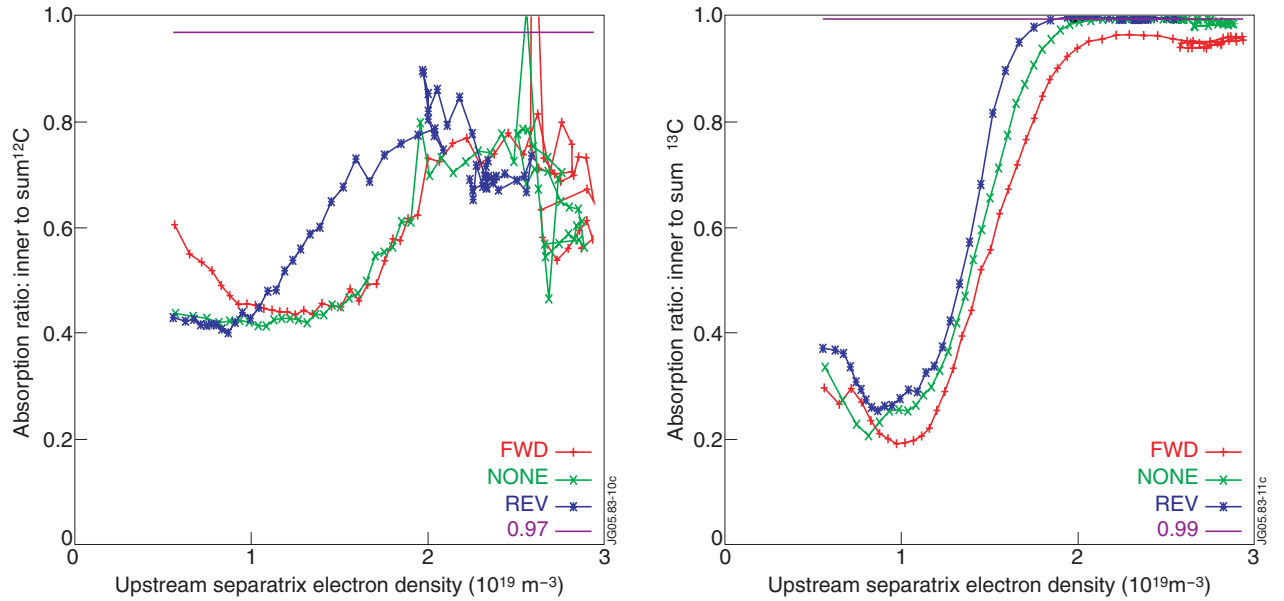

Figure 7: Absorption ratio for 12C (left) and 13C (right) for the inner target to sum of both targets for the cases in figure 5. The magenta lines indicate experimental estimates of the asymmetry.